iScience

CellPress
OPEN ACCESS

Article

SFTSV infection is associated with transient overproliferation of monoclonal lambda-type plasma cells

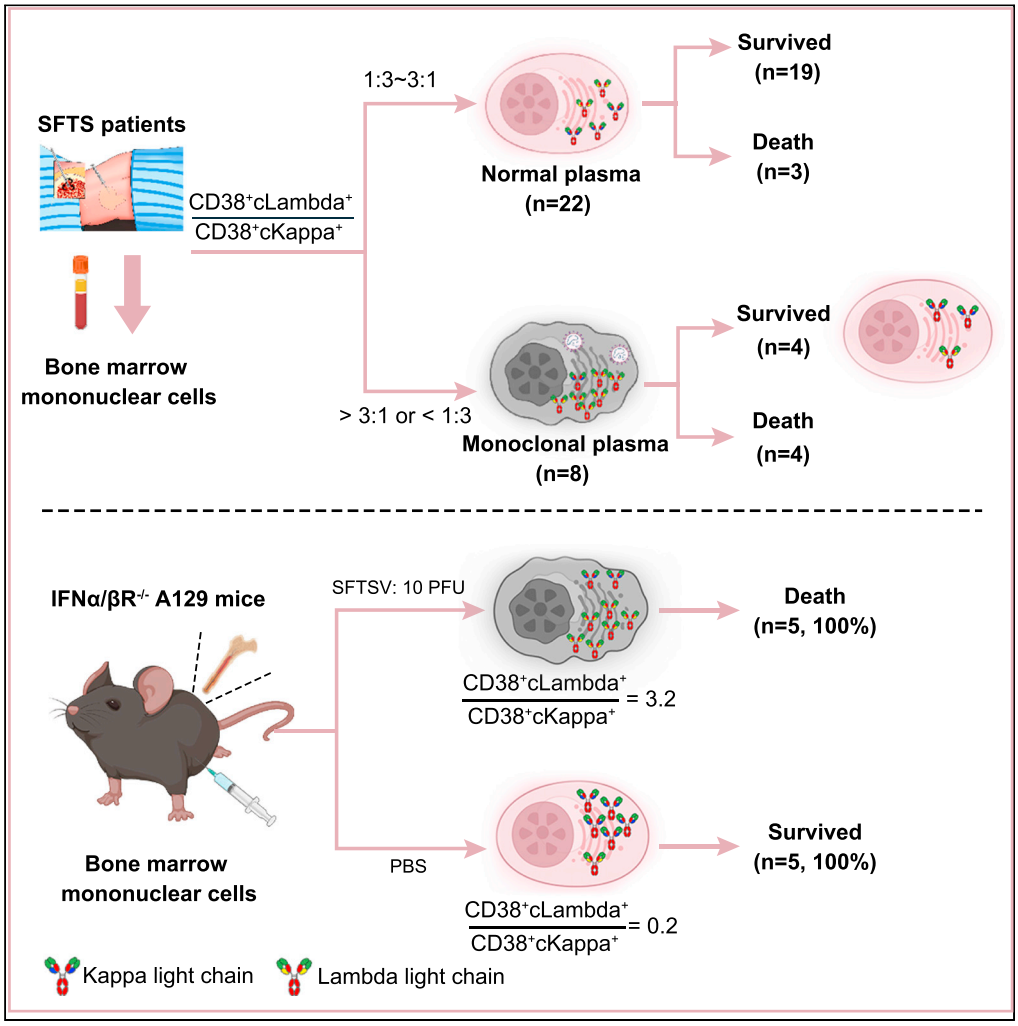

Chuansong Quan, Qinghua Liu, Lijuan Yu, ..., Michael J. Carr, Hong Zhang, Weifeng Shi

tyfyzhh@163.com (H.Z.)
shiwf@ioz.ac.cn (W.S.)

Highlights

The lambda-type monoclonal plasma cells in bone marrow were observed in SFTS cases

Monoclonal plasma subsets were positively correlated with clinical severity

The number of plasma cells dropped to near normal levels in recovered MCP cases

Phenotype of MCP cells was found in the bone marrow of SFTSV-infected mice

Quan et al., iScience 26, 106799
June 16, 2023
https://doi.org/10.1016/j.isci.2023.106799

iScience

CellPress
OPEN ACCESS

Article

SFTSV infection is associated with transient overproliferation of monoclonal lambda-type plasma cells

Chuansong Quan,[1,2,11] Qinghua Liu,[3,11] Lijuan Yu,[2,11] Chunjing Li,[4,11] Kaixiao Nie,[2] Guoyong Ding,[5] Hong Zhou,[2] Xinli Wang,[6] Wenwen Sun,[6] Huiliang Wang,[1] Maokui Yue,[7] Li Wei,[8] Wenjun Zheng,[2] Qiang Lyu,[5] Weijia Xing,[5] Zhenjie Zhang,[2] Michael J. Carr,[9,10] Hong Zhang,[1,4,*] and Weifeng Shi[2,5,12,*]

SUMMARY

The impairment of antibody-mediated immunity is a major factor associated with fatal cases of severe fever with thrombocytopenia syndrome (SFTS). By collating the clinical diagnosis reports of 30 SFTS cases, we discovered the overproliferation of monoclonal plasma cells (MCP cells, $CD38^{+}cLambda^{+}cKappa^{-}$) in bone marrow, which has only been reported previously in multiple myeloma. The ratio of $CD38^{+}cLambda^{+}$ versus $CD38^{+}cKappa^{+}$ in SFTS cases with MCP cells was significantly higher than that in normal cases. MCP cells presented transient expression in the bone marrow, which was distinctly different from multiple myeloma. Moreover, the SFTS patients with MCP cells had higher clinical severity. Further, the overproliferation of MCP cells was also observed in SFTS virus (SFTSV)-infected mice with lethal infectious doses. Together, SFTSV infection induces transient overproliferation of monoclonal lambda-type plasma cells, which have important implications for the study of SFTSV pathogenesis, prognosis, and the rational development of therapeutics.

INTRODUCTION

Severe fever with thrombocytopenia syndrome (SFTS), caused by the SFTS virus (SFTSV) in the order *Bunyavirales*, is an emerging, high-consequence, tick-borne pathogen with a case fatality rate ranging from 12% to 50%.[1,2] SFTSV poses a serious threat to public health in East Asia, and the related Heartland virus has also been reported in the United States.[3,4] The host spectrum of SFTSV continues to expand, including ticks, humans, livestock animals, and domesticated pets (e.g., cats and dogs).[5] SFTS is one of the top-scoring diseases in the World Health Organization (WHO) annual review in 2019 that warrant accelerated research and development due to the absence of effective prophylactic and therapeutic measures.[6]

Clinical manifestations of SFTS vary greatly between patients and usually include fatigue, myalgia, and gastrointestinal symptoms, such as lack of appetite, nausea, vomiting, and diarrhea, which are accompanied by thrombocytopenia, leukocytopenia, and lymphadenopathy.[7,8] A typical course of SFTSV infection generally has four distinct phases: incubation, fever, multiple organ failure, and convalescence.[9] Multiple organ failure develops rapidly, and this phase is characterized by an abrupt increase in biomarkers, such as aspartate aminotransferase (AST), creatine kinase (CK), and lactate dehydrogenase (LDH).[10] These clinical symptoms, however, are similar to those of anaplasmosis, hemophagocytic lymphohistiocytosis, and acute leukemia and can lead to clinical misdiagnoses.[11]

Although the pathogenesis of SFTSV remains unclear, recent studies have shed light on the immunological mechanisms in fatal SFTS cases.[12–17] SFTSV can infect monocytes leading to apoptosis, diminish antigen presentation, inhibit T cell activation, and block the isotype-switched antibody response.[16] Importantly, SFTSV can directly infect B cell populations—principally plasmablast and plasma cells—resulting in the deregulation of B cell composition and the disruption of B cell-mediated humoral immunity resulting in ineffective neutralizing antibodies, which represent a hallmark of fatal SFTS cases.[15–17] Additionally, high viral loads, hyperinflammatory responses, and aberrant complement activation have also been reported in critical SFTS cases.[12–14] Recent reports have also profiled B cell immunity in the peripheral blood

[1]Department of Infectious Disease, The Second Affiliated Hospital of Shandong First Medical University, Taian 271000, China

[2]Key Laboratory of Emerging Infectious Diseases in Universities of Shandong, School of Clinical and Basic Medical Sciences, Shandong First Medical University & Shandong Academy of Medical Sciences, Taian, 271000, China

[3]Department of Clinical Laboratory, The Second Affiliated Hospital of Shandong First Medical University, Taian 271000, China

[4]Department of Hematology, The Second Affiliated Hospital of Shandong First Medical University, Taian 271000, China

[5]School of Public Health, Shandong First Medical University & Shandong Academy of Medical Sciences, Ji'nan 250117, China

[6]Department of Pathology, The Second Affiliated Hospital of Shandong First Medical University, Taian 271000, China

[7]Department of Critical Care Medicine, The Second Affiliated Hospital of Shandong First Medical University, Taian 271000, China

[8]Department of Respiratory Medicine, The Second Affiliated Hospital of Shandong First Medical University, Taian 271000, China

[9]National Virus Reference Laboratory, School of Medicine, University College Dublin, Dublin 4, Ireland

Continued

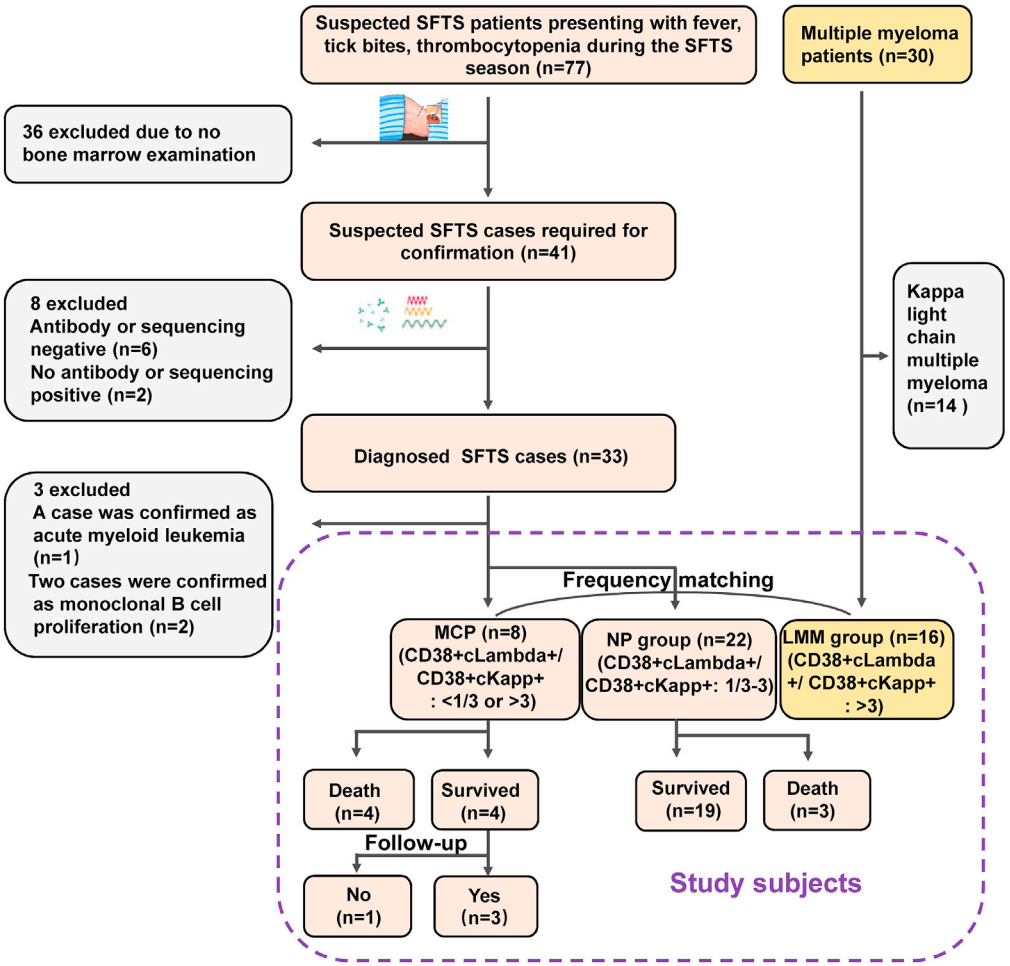

Figure 1. Flow chart of SFTS and LMM patients enrolled in the study

The classification of suspected severe fever with thrombocytopenia syndrome (SFTS) cases from hematologic diseases between April 2018 to May 2022 at the Second Affiliated Hospital of Shandong First Medical University. LMM: lambda light chain multiple myeloma; MCP: monoclonal plasma cells with overexpressed lambda chains; NP: normal plasma.

mononuclear cells (PBMCs) in SFTSV-infected patients[16,18]; however, the characterization of plasma cells from the bone marrow of SFTSV cases remains less well understood. Importantly, it is crucial to understand how humoral immunity developing in bone marrow mitigates against SFTSV infection and to assess the plasma cell changes for timely clinical diagnosis and treatment.

Herein, we have collated and analyzed the clinical diagnosis reports of 30 SFTS patients, discovering over-proliferation of a subset of myeloma-like monoclonal plasma cells (MCP cells; $CD38^{+}cLambda^{+}cKappa^{-}$) in the bone marrow of eight SFTS patients. Meanwhile, we further explored whether the frequency of MCP cells affected prognosis, decreased the titer of virus-specific antibodies, and could persist in a comparable manner to multiple myeloma. In addition, overproliferation of MCP cells was also observed in challenged mice. Collectively, we have elucidated systematically the characteristics of MCP cells associated with SFTSV infection.

RESULTS

Characteristics of the study participants

77 suspected SFTS patients were retrospectively assessed from April 2018 to May 2022 at the Second Affiliated Hospital of Shandong First Medical University (Figure 1). Among them, 33 cases with bone marrow examination tested positive for SFTSV by quantitative RT-PCR (n = 22), serological detection (n = 6), virus

[10]International Collaboration Unit, International Institute for Zoonosis Control, Hokkaido University, N20 W10 Kita-ku, Sapporo 001-0020, Japan

[11]These authors contributed equally

[12]Lead contact

*Correspondence: tyfyzhh@163.com (H.Z.), shiwf@ioz.ac.cn (W.S.)

https://doi.org/10.1016/j.isci.2023.106799

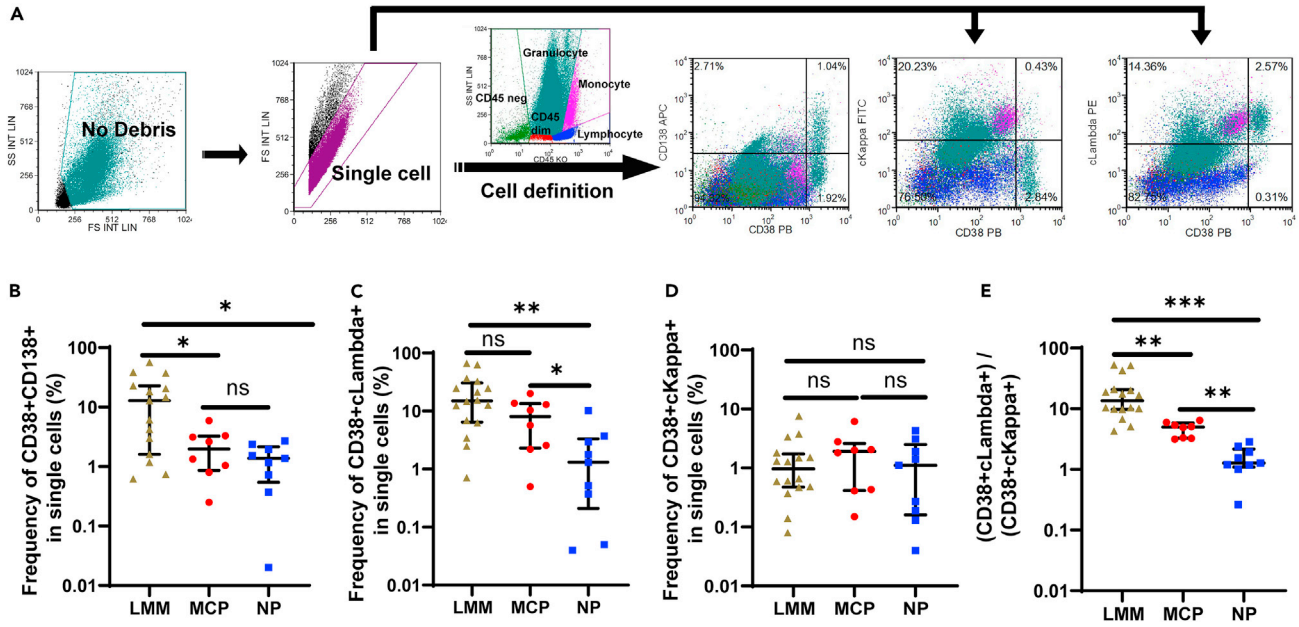

Figure 2. Characterization of plasma cell subsets in the marrow from SFTS and LMM patients

(A) FACS gating strategy for measurement of plasma cell subsets. Plasma cells ($CD38^+CD138^+$) and monoclonal plasma cells with cytoplasmic lambda light chain ($CD38^+cLambda^+$) and ($CD38^+cKappa^-$).

(B–D) The frequency of different plasma cell subsets from LMM and SFTS bone marrow lymphocytes.

(E) The ratio of $CD38^+cLambda^+/CD38^+cKappa^+$ in total cell in three groups. LMM: lambda light chain multiple myeloma; MCP: SFTS patients with monoclonal plasma cells; NP: SFTS patients with normal plasma cells. The median (IQR) is shown for each group, and the differences between two groups were tested by *t* test for normally distributed data or Mann-Whitney test for non-normally distributed variables. Owing to the frequency of CD38 within the normal range (<0.5%), plasma cell phenotypes were not further detected, and 9 from 22 SFTS cases with normal plasma cells were used for analysis in the NP group. Statistical significance was represented by asterisks, *$p < 0.05$, **$p < 0.01$, ***$p < 0.001$.

isolation (n = 6), or next-generation sequencing (n = 2; Table S1). Three cases were excluded from the following analyses, including two with monoclonal B cell proliferation and one with acute myeloid leukemia. The remaining 30 cases included 13 female cases (43.3%), and the median age was 64.0 years (interquartile range [IQR] 56.5–74.2 years). The median time of symptom onset was 5 days (IQR 4–7 days), and there were seven (23.3%) fatal cases (Figure S1).

According to the ratio of lambda/kappa chain in the cytoplasm (cLambda/cKappa), the 30 SFTS patients were divided into two groups: an MCP group (>3:1, n = 8) and a normal plasma (NP) group (between 1:3 and 3:1, n = 22; Figure 1). As the occurrence of MCP cells in SFTS patients was a similar phenotype to those with lambda light chain multiple myeloma patients (LMMs), 16 LMMs with age- and sex-frequency matching were recruited to compare the differences between the MCP cases and multiple myeloma patients. The median age of LMMs was 65.0 years (IQR 54.5–70.0 years), and 9 cases (56.3%) were female (Table S2).

Occurrence of MCP cells in the bone marrow of SFTS cases

To identify potential hematologic diseases, bone marrow aspiration, biopsy for immunohistochemistry (IHC), and cellular phenotype analysis by flow cytometry were performed. Single cells in the bone marrow were divided into granulocytes, monocytes, and lymphocytes on the basis of CD45 expression (Figure 2A). The frequency of $CD38^+CD138^+$ plasma cells in the LMM group (median 12.8%, IQR 1.6–22.8%) was higher than that in the MCP (median 2.0%, IQR 0.9–3.2%, $p = 0.03$) and NP groups (median 1.4%, IQR 0.5–2.1%, $p = 0.006$; Figure 2B). For the $CD38^+cLambda^+$ subset, the frequency in the LMM (median 15.0%, IQR 6.4–30.4%, $p = 0.001$) and MCP group (median 8.0%, IQR 2.3–13.5%, $p = 0.03$) was higher than that in the NP group (median 1.3%, IQR 0.2–3.3%), yet there were no significant differences between the MCP and LMM groups ($p = 0.1$; Figure 2C). Similarly, the frequency of $CD38^+cKappa^+$ subset did not differ significantly among the three groups (all $p > 0.05$; Figure 2D). However, the ratio of $CD38^+cLambda^+$ versus $CD38^+cKappa^+$ in the LMM (median 13.5, IQR 9.8–20.7, $p < 0.01$) and MCP groups (median 5.0, IQR

3.3–5.8, $p < 0.01$) was significantly higher than that of NP group (median 1.3, IQR 1.1–2.2; Figure 2E), suggesting the MCP cells presented in the bone marrow of the SFTS cases were monoclonal lambda-type plasma cells. Similar results were obtained using the Brown-Forsythe ANOVA test with Games-Howell's multiple comparisons (Figure S2). Hence, these results revealed that SFTSV infection was likely to cause overproliferation of monoclonal lambda-type plasma cells ($CD38^{+}cLambda^{+}cKappa^{-}$) in a subset of SFTS patients.

In order to visualize the characterization of the MCP cells, IHC was performed on the bone marrow samples from acute SFTS cases. The results of typical SFTS cases showed that B cell markers (CD19 or CD20) were rarely detected in the bone marrow samples in the acute phase of the SFTS patients, such as in cases 6 and 24 (Figure S3A), whereas plasma cells stained with CD38 and CD138 cellular markers were abundant in the bone marrow (Figure S3A). The cLambda and cKappa chains are two important functional cellular markers located in the cytoplasm.[19] Notably, the expression of the cLambda light chain in the cytoplasm of plasma cells was highly upregulated in the bone marrow of case 6 (an acute SFTS case), while the cKappa light chain was rarely detected in the cytoplasm (Figure S3A), suggesting that the lambda light chain gene expression may be affected by SFTSV infection. Double immunofluorescence staining for CD38 and lambda cellular markers was performed to further characterize the plasma cells in the bone marrow, and the results demonstrated that the CD38 and lambda markers were co-expressed in plasma cells, and both the count and fluorescence intensity of cLambda light chain in case 6 were stronger than those in case 24 with normal plasma cells (Figure S3B). Hence, these results further confirmed that SFTSV infection could cause overproliferation of monoclonal lambda-type plasma cells similar to lambda light chain multiple myeloma.

We obtained the peripheral blood single-cell data from seven SFTS patients (20,207 cells) and identified 13 cells containing SFTSV sequences, including six cells annotated as B or plasma cells. Two cells from case P19 of the NP group harbored 105 virus reads, and the counts of the *immunoglobulin lambda chain* (*IGLC*) genes were 75. The other four cells from case P6 of the MCP group contained 41 virus reads, and the counts of the *IGLC* genes were 533, which showed that SFTSV-infected plasma cells could induce higher expression of the lambda light chain (Table S3). Furthermore, comparison between SFTSV-infected and non-infected cells found that the expression of *IGLC2* in virus-infected cells was significantly higher than that in virus-uninfected cells ($p < 0.05$), while there was no statistically significant difference in the expression of *immunoglobulin kappa chain* (*IGKC*) between the two groups (Figure S4). To further explore these findings, we have reanalyzed the single-cell data from a prior SFTSV study[17] and compared the gene expression between 23 plasma cells/plasmablasts containing viral sequences and 2,028 non-virus-infected B cells from two dead patients (NCBI GEO database: GSE149313). We found that *IGLC3*, *IGLC6*, *IGLC7*, and *IGKC* were among the top 20 differentially expressed genes, and the read counts of *IGLC3* in SFTSV-infected cells were significantly higher than those in the uninfected cells (median: 178.5, IQR: 22.2–3190 vs. median: 17, IQR: 3–171, $p = 5.60957E\text{-}32$; Figure S5). These data provide evidence that SFTSV infection could cause overproliferation of monoclonal lambda-type plasma cells.

Monoclonal plasma subsets were positively correlated with clinical severity in the SFTS patients

To examine the relationship between the MCP cells and clinical outcomes, the indices of hematological analysis, coagulation tests, liver function tests, renal function tests, and cardiology examination were systematically analyzed for the SFTS cases in both the MCP and NP groups. Four out of eight (50.0%) patients in the MCP group died, while only three out of 22 (13.6%) died in the NP group ($p = 0.04$, Table 1). Levels of liver enzymes in the MCP group, including alanine aminotransferase (ALT, median 334.0, IQR 146.0–376.8, $p < 0.01$) and aspartate aminotransferase (AST, median 661.5, IQR 469.5–916.0, $p < 0.01$), were significantly higher than those in the NP group, and the concentrations of LDH (median 1868.0, IQR 1145.0–3601.0, $p < 0.01$) and CK (median 1480.0, IQR 468.0–8492.0, $p = 0.02$) related to heart and kidney function were also significantly increased (Table 1), suggesting that SFTS cases with MCP cells were more likely to develop acute multiple organ injuries. Although SFTSV infection affected the clotting process and changed the composition of lymphocytes, there were no significant differences in the albumin (ALB), activated partial thromboplastin time (APTT), blood urea nitrogen (BUN), creatinine (CRE), D-dimer, fibrinogen (FIB), hemoglobin (HGB), lymphocyte, platelet (PLT), prothrombin time (PT), red blood cell (RBC), total bilirubin (TBIL), white blood cell (WBC), and β2-microglobulin (β_2-MG) between the two groups (Table 1). Notably, these indices in both the MCP and NP groups greatly exceeded the normal reference ranges, and they were

Table 1. Clinical outcomes and diagnosis of SFTS cases

Characteristics	MCP (n = 8)	NP (n = 22)	P^a
Death, n (%)	4 (50%)	3 (13.6%)	**0.04**
ALT (U/L; normal range: 5–50)	334.0 (146.0–376.8)	71.5 (35.0–68.5)	**<0.01**
AST (U/L; normal range:14–40)	661.5 (469.5–916.0)	143.5 (97.2–246.5)	**<0.01**
LDH (U/L; normal range:120–250)	1868.0 (1145.0–3601.0)	654.0 (368.0–897.3)	**<0.01**
CK (U/L; normal range: 50–310)	1480.0 (468.0–8492.0)	400.0 (152.0–1324.0)	**0.02**
RBC($\times10^{12}$/L; normal range: 3.5–5)	4.5 (4.4–4.8)	4.5 (4.0–4.8)	0.49
WBC ($\times10^9$/L; normal range: 4–10)	1.4 (1.3–2.7)	1.8 (1.1–3.2)	0.07
PLT ($\times10^9$/L; normal range: 100–300)	53.0 (42.0–88.0)	60.0 (32.0–77.0)	0.63
HGB (g/L; normal range: 110–150)	129.3 (136.0–151.5)	133.5 (126.0–149.8)	0.68
Lymphocytes ($\times10^9$/L; normal range: 0.8–4)	0.33 (0.32–0.79)	0.47 (0.34–0.80)	0.34
PT (s; normal range: 10.5–15)	11.8 (10.6–12.0)	12.0 (10.5–13.0)	0.69
APTT (s; normal range: 22–38)	39.4 (37.3–43.0)	38.4 (32.7–48.9)	0.95
D-dimer (mg/L; normal range: 0–0.5)	7.4 (5.0–30.2)	4.1 (1.5–11.6)	0.08
FIB (g/L; normal range: 2–4)	1.8 (1.5–2.1)	2.2 (1.7–2.6)	0.15
TBIL (μmol/L; normal range: 2–25)	7.6 (6.0–10.6)	8.5 (6.5–11.2)	0.51
ALB (g/L; normal range: 40–55)	30.6 (26.2–35.6)	34.1 (29.6–36.0)	0.23
CR (μmol/L; normal range:57–97)	67.4 (52.4–82.2)	69.8 (62.7–99.1)	0.46
BUN (mmol/L; normal range: 3.1–8.8)	5.4 (4.5–7.6)	5.7 (4.5–8.8)	0.67
β_2-MG (mg/L; normal range:0.8–2.8)	3.6 (2.8–4.7)	4.1 (3.5–5.7)	0.26

Data are n (%) or median (IQR). Abbreviations: ALB, albumin (g/L); ALT, alanine transaminase (U/L); APTT, activated partial thromboplastin time (s); AST, aspartate aminotransferase (U/L); BUN, blood urea nitrogen (mmol/L); CK, creatine Kinase(U/L); CR, creatinine (μmol/L); D-dimer (mg/L); FIB, fibrinogen (g/L); HGB, hemoglobin (g/L); IQR, interquartile range; LDH, lactate dehydrogenase (U/L); PLT, platelet counts ($\times10^9$/L); PT, prothrombin time (s); RBC, red blood cell ($\times10^9$/L); TBIL, total bilirubin (umol/L); WBC, white blood cell ($\times10^9$/L); β_2-MG, β2-microglobulin (mg/L). Characteristics of clinical indicators were determined at first hospitalization presentation.

[a]*P* values were calculated by Mann-Whitney test or *t* test, as appropriate. Significant p values are shown in bold.

also significantly different between the MCP and LMM groups, with the exception of BUN, CRE, PT, TBIL, and β_2-MG measurements (Table S4).

Furthermore, we performed a correlation analysis and discovered that the ratio of $CD38^+cLambda^+$/$CD38^+cKappa^+$ was positively correlated with concentrations of ALT ($r_s = 0.68$, $p < 0.001$), AST ($r_s = 0.66$, $p < 0.001$), and LDH ($r_s = 0.62$, $p < 0.001$; Figures S6A–S6C). In addition, the $CD38^+CD138^+$ plasma subset was also correlated with levels of globulin (GLO, $r_s = 0.44$, $p = 0.015$) and LDH ($r_s = 0.40$, $p = 0.028$; Figures S6D and S6E), yet the frequency of plasma cells had no correlation with other clinical indicators (Table S5). These results suggested that overproliferation of monoclonal lambda-type plasma subsets in SFTS cases might be related with severe organ injury and clinical outcome.

To assess the systemic inflammatory response between the MCP cells and clinical outcomes, we obtained the peripheral blood single-cell transcriptomics data from seven SFTS patients (20,207 cells), including one MCP case and five NP cases. The differentially expressed genes between MCP and NP cases were analyzed, and the expression of several cytokine/chemokine related genes, such as *interleukin 2 receptor subunit beta* (*IL-2RB*), *interleukin 2 receptor subunit gamma* (*IL-2RG*), interleukin 7 receptor (*IL-7R*), *chemokine* (*C-C motif*) *ligands 4* (*CCL-4*), and *interferon gamma receptor 1* (*IFNGR1*), was found to be distinctly increased in the MCP patients (Figure S7). In addition, we tested four typical cytokines/chemokines (IL-1Ra, IL-6, IFN-γ and macrophage inflammatory proteins (MIP)-1β) previously reported to be associated with SFTS disease severity.[20] The plasma from bone marrow of the SFTS cases (including 4 MCP and 7 NP cases) was tested by enzyme-linked immunosorbent assay (ELISA). The results showed that the optical density 450 (OD_{450}) of IL-6 was 0.30 ± 0.15 in MCP group, which was significantly higher than that in NP group (0.15 ± 0.06, p = 0.015). However, the OD_{450} of IFN-γ, IL-1Ra, and MIP-1β only had a higher trend in measurements between the MCP and NP groups, likely due to the small sample size (Figure S8). These results indicated that MCP patients have more severe inflammatory responses compared to the NP cases.

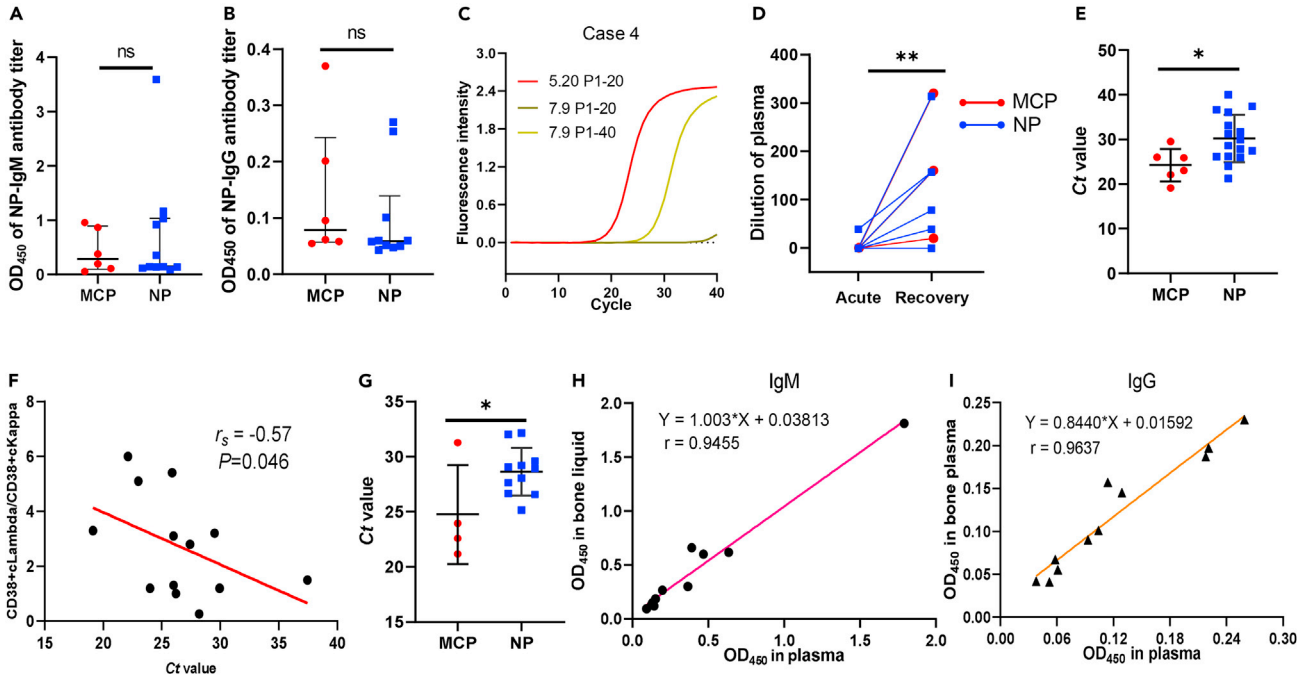

Figure 3. The viral loads and antibody responses to the SFTSV nucleocapsid protein in both plasma and marrow liquid

(A and B) The NP-specific IgM and IgG antibody titers in plasma among MCP and NP groups were diluted in 1:10 and 1:100, and OD_{450} measurements were determined by a commercial ELISA kit.

(C) The neutralization titers for different time points for the representative case 4 were recorded by real-time quantitative RT-PCR. The red, brown, and green curves represented collection date 2020.5.20 diluted 1: 20, collection date 2020.7.9 diluted 1: 20, and collection date 2020.7.9 diluted 1: 40, respectively.

(D) Neutralization antibodies in acute or recovery phase plasma in paired samples were tested by 2-fold dilutions in the range 1:20-640, and paired *t* test was used for statistical analysis. The red and blue lines represent the MCP and NP groups, respectively.

(E) Plasma viral loads of each acute phase patient were determined by real-time quantitative RT-PCR, and cycle threshold (*Ct*) values between the MCP and NP groups were compared.

(F) Spearman's correlation coefficients were calculated between plasma viral load (*Ct* value), and the ratio of $CD38^+cLambda^+$ versus $CD38^+cKappa^+$ using viremic samples. X axis denotes the *Ct* value in plasma. r_s and *P* indicate the correlation coefficient and significance, respectively.

(G) Viral loads in the bone marrow lymphocytes of each acute phase patient were determined by real-time quantitative RT-PCR, and cycle threshold (*Ct*) values between the MCP and NP groups were compared.

(H and I) Correlation of NP-specific IgM and IgG antibody levels between plasma and bone liquid. The differences between two groups were tested by Mann-Whitney test or *t* test, as appropriate. r_s indicates the Spearman correlation coefficient. Statistical significance was represented by an asterisk, *p < 0.05; **p < 0.01; ns, no significance.

Plasma antibody response against SFTSV

To test whether the presence of MCP cells affects virus-specific antibody levels and their function, we employed ELISA and virus neutralization to detect NP-specific IgM/IgG and neutralizing antibodies in blood plasma and marrow liquid. There were no significant differences in NP-specific IgM or IgG in the plasma between the MCP and NP cases during the acute phase (p = 0.73, p = 0.27; Figures 3A, 3B, and Table S1). Similarly, the seroconversion rates of both groups were similar (100% versus 71.4%, p = 1; Table S1), and the geometric mean titers (GMTs) of protective neutralizing antibodies in convalescent plasma were significantly elevated in the SFTS patients from 6.3 (±2) to 80.0 (±4) (p = 0.008; Figures 3C, 3D, and Table S1). To investigate whether viremia affected the presence of MCP cells in SFTS patients, the viral loads in the plasma were determined by quantitative RT-PCR, and mean *Ct* value was 24.2 (±3.6) in the MCP group, which was lower (higher viral load) than that in the NP group (30.2 ± 5.3, p = 0.02; Figure 3E). Meanwhile, the ratio of $CD38^+cLambda^+/CD38^+cKappa^+$ had a strong inverse association (Spearman's $r_s = -0.57$, p = 0.046) with plasma viral load as demonstrated by the correlation analysis in SFTS cases (Figure 3F and Table S1). Quantitative RT-PCR detection was performed on the bone marrow lymphocytes, and we found that the *Ct* value of viral load in them was 24.7 ± 4.5, while that of normal plasma cells was 28.6 ± 2.1 (p = 0.037; Figure 3G). In addition, the antibody levels of NP-specific IgM and IgG in blood plasma and marrow liquid had a strong positive correlation (IgM: *r* = 0.95, IgG: *r* = 0.96; Figures 3H and 3I), suggesting the binding antibodies in the plasma could indeed be used to estimate the antibody level in the bone marrow.

SFTSV infection induced transient overproliferation of MCP cells

To answer the question whether the appearance of MCP cells was persistent in the SFTS cases like those in the LMM group, we had a follow-up visit with three surviving SFTS patients with MCP cells between 56 and 152 days after symptom onset. Although the plasma subsets ($CD38^+CD138^+$) in the bone marrow varied across the three individuals with paired samples, they generally had a decreasing trend, while non-plasma subsets ($CD38^-CD138^-$) significantly increased along the recovery process of SFTS ($p < 0.01$, Figure 4A). The median frequency of $CD38^+clambda^+$ plasma cells was 12.9% (IQR 10.4–13.7%) in the acute phase, while it sharply declined to 0.7% (IQR 0.3–1.6%) in the recovery phase ($p < 0.01$, Figure 4B). Meanwhile, the frequency of $CD38^+cKappa^-$ subtype (median 13.8%, IQR 9.5–17.0%) decreased to 2.3% (IQR 0.2–2.3%) after recovery of the SFTS cases ($p = 0.02$, Figure 4C). Consistently, the ratio of $CD38^+cLambda^+$ versus $CD38^+cKappa^+$ declined rapidly from the acute phase (median 5.0, IQR 4.9–6.4) transition to the recovery phase (median 0.8, IQR 0.6–0.9, $p = 0.01$) and reduced to the normal range (Figure 4D). These findings suggested that the number of plasma cells dropped to near-normal levels after the SFTS patients recovered, and MCP cells presented transient expression in the bone marrow, which revealed that the occurrence of MCP cells was distinctly different from multiple myeloma.

Phenotype of MCP cells was found in the bone marrow of SFTSV-infected mice

Animal experiments were performed to further explore the overproliferation phenotype of MCP cells in the bone marrow caused by SFTSV infection. Preliminary animal infection experiments showed the clinical severity in the type I IFN alpha/beta receptor ($IFN\alpha/\beta R^{-/-}$) gene-deficient A129 mice was infection dose dependent (supplemental materials, Figure S9).

The lymphocytes were gated from bone marrow, and the frequency of plasma cell subsets was analyzed (Figure 5A). Although the proportion of the $CD38^+CD138^+$ subset in the 10 plaque-forming units (PFUs) group was not significantly different from that of other groups ($p > 0.05$), the 2 PFU group (median 4.4%, IQR 2.6–5.9%) had a higher proportion than the 0.08 PFU (median 1.1%, IQR 1.0–1.7%, $p < 0.01$) and phosphate-buffered saline (PBS) group (median 0.7%, IQR 0.5–1.2%, $p < 0.01$; Figure 5B). However, the number of plasma cells of the $CD38^+cLambda^+$ subset in the 10 PFU group (median 15.5%, IQR 6.6–23.2%) was much higher than that in the 0.4 PFU (median 1.2%, IQR 0.8–2.8%, $p < 0.01$), 0.08 PFU (median 1.3%, IQR 1.0–1.8%, $p < 0.01$), and PBS groups (median 1.0%, IQR 0.7–1.3%, $p < 0.01$; Figure 5C), yet the frequency of $CD38^+cKappa^+$ subset had no difference among groups (all $p > 0.05$; Figure 5D). As expected, the ratio of $CD38^+cLambda^+/CD38^+cKappa^+$ in the 10 PFU group (median 3.2, IQR 1.7–6.0) was significantly higher than that in the 2 PFU (median 0.6, IQR 0.4–2.9, $p = 0.04$), 0.4 PFU (median 0.6, IQR 0.3–1.0, $p < 0.01$), 0.08 PFU (median 0.2, IQR 0.2–0.5, $p < 0.01$), and PBS groups (median 0.2, IQR 0.1–0.2, $p < 0.01$; Figure 5E). These results suggested the frequency of plasma cells and the ratio of $CD38^+cLambda^+/CD38^+cKappa^+$ increased significantly with increasing infectious dose, particularly in the $CD38^+cLambda^+$ subset. To exemplify the dynamic changes of MCP cells, the frequency of $CD38^+CD138^+$ (1.6%–2.9%) and $CD38^+cLambda^+$ (1.9%–15.5%) subsets increased from 3 dpi to 5 dpi in the 10 PFU group, while the frequency of $CD38^+cKappa^+$ showed a significant decrease (10.9%–4.8%; Figures 5F–5H). Meanwhile, the ratio of $CD38^+cLambda^+/CD38^+cKappa^+$ increased from 0.2 to 3.2 from 3 dpi to 5 dpi ($p = 0.03$; Figure 5I). These results further indicated that overproliferation of the monoclonal lambda-type plasma cells were more likely to occur in the bone marrow in the acute phase of severe SFTS cases.

The association between occurrence of MCP and SFTSV genotyping

To answer whether the appearance of MCP cells was associated with the SFTSV subtyping, we performed next-generation sequencing and obtained full-length genome sequences from two MCP (P2 and P6) and three NP (P11, P24, and P28) cases. Phylogenetic analyses showed that SFTSV strains from the two MCP cases, two NP cases (P11 and P28), and the challenge strain used for animal experiments fell within genotype C3 in the phylogenetic trees constructed using the L, M, and S genes, respectively (Figure S10). Whether SFTSV strains of other genotypes could induce the appearance of MCP cells warrants further study.

DISCUSSION

Overproliferation of MCP cells is common in plasma cell neoplasms, such as multiple myeloma, Waldenstrom's macroglobulinemia, and systemic amyloidosis.[21–24] To our knowledge, the occurrence of an overproliferation of MCP cells caused by viral infection has previously not been reported systematically from

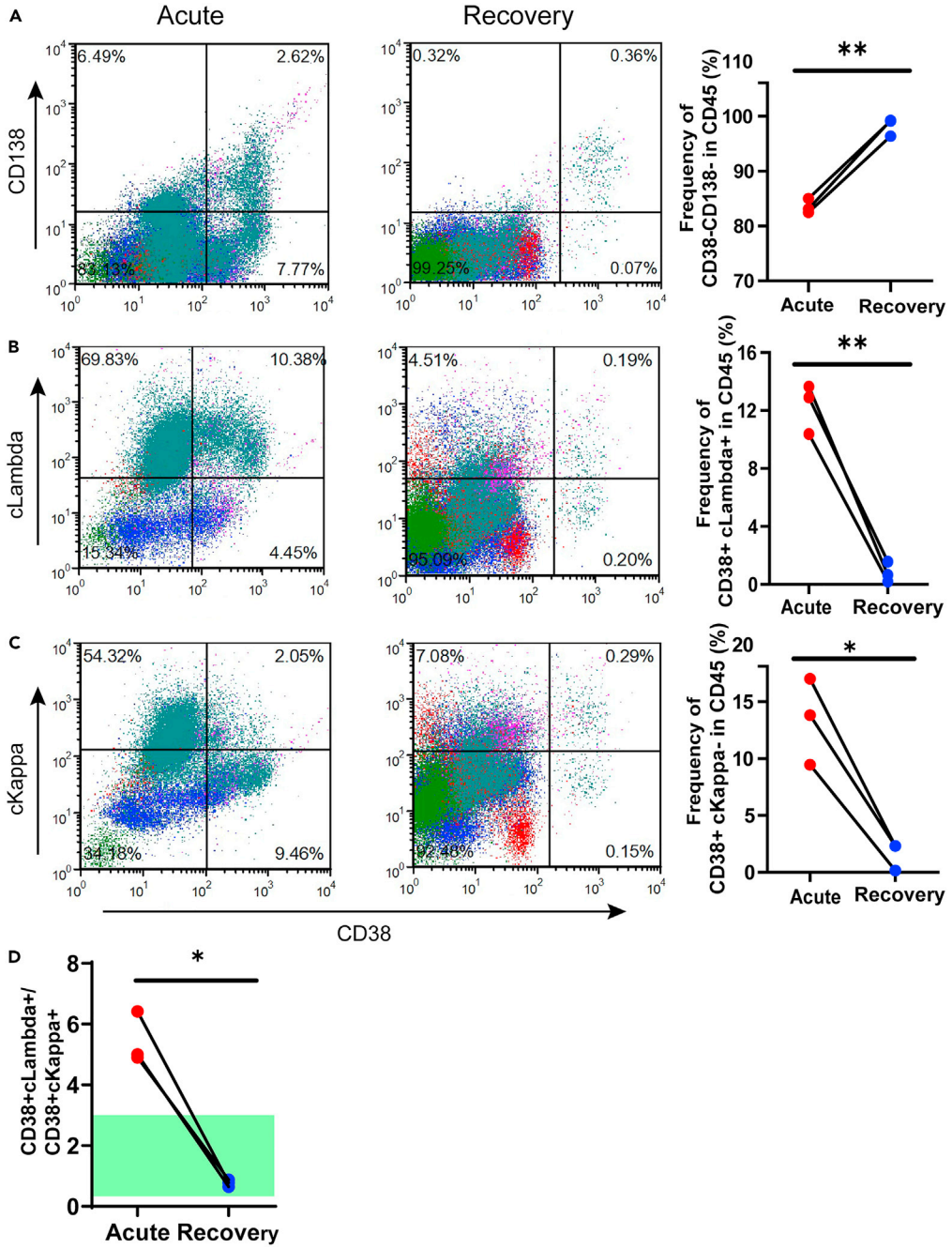

Figure 4. SFTSV infection induces transient overproliferation of MCP cells

(A–C) The changes of different plasma subsets ($CD38^+CD138^+$, $CD38^+cLambda^+$, and $CD38^+cKappa^+$) in both the acute and recovery phases in SFTS cases. The changes of different plasma subsets in both the acute and recovery phases for the representative MCP case 6 are shown, and paired *t* tests were employed to assess the significance.

(D) The ratio of $CD38^+cLambda^+/CD38^+cKappa$ in the acute and recovery phases was compared, and paired *t* test was used to assess the significance. The green shade represents the normal region. Statistical significance was represented by asterisks, *$p < 0.05$, **$p < 0.01$.

bone marrow. In the present study, clinical samples were collected from 30 acute SFTS patients between April 2018 and May 2022 to analyze the phenotypic changes of bone marrow lymphocytes, especially the B cell subsets that mediate the humoral immune responses. Surprisingly, overproliferation of the monoclonal

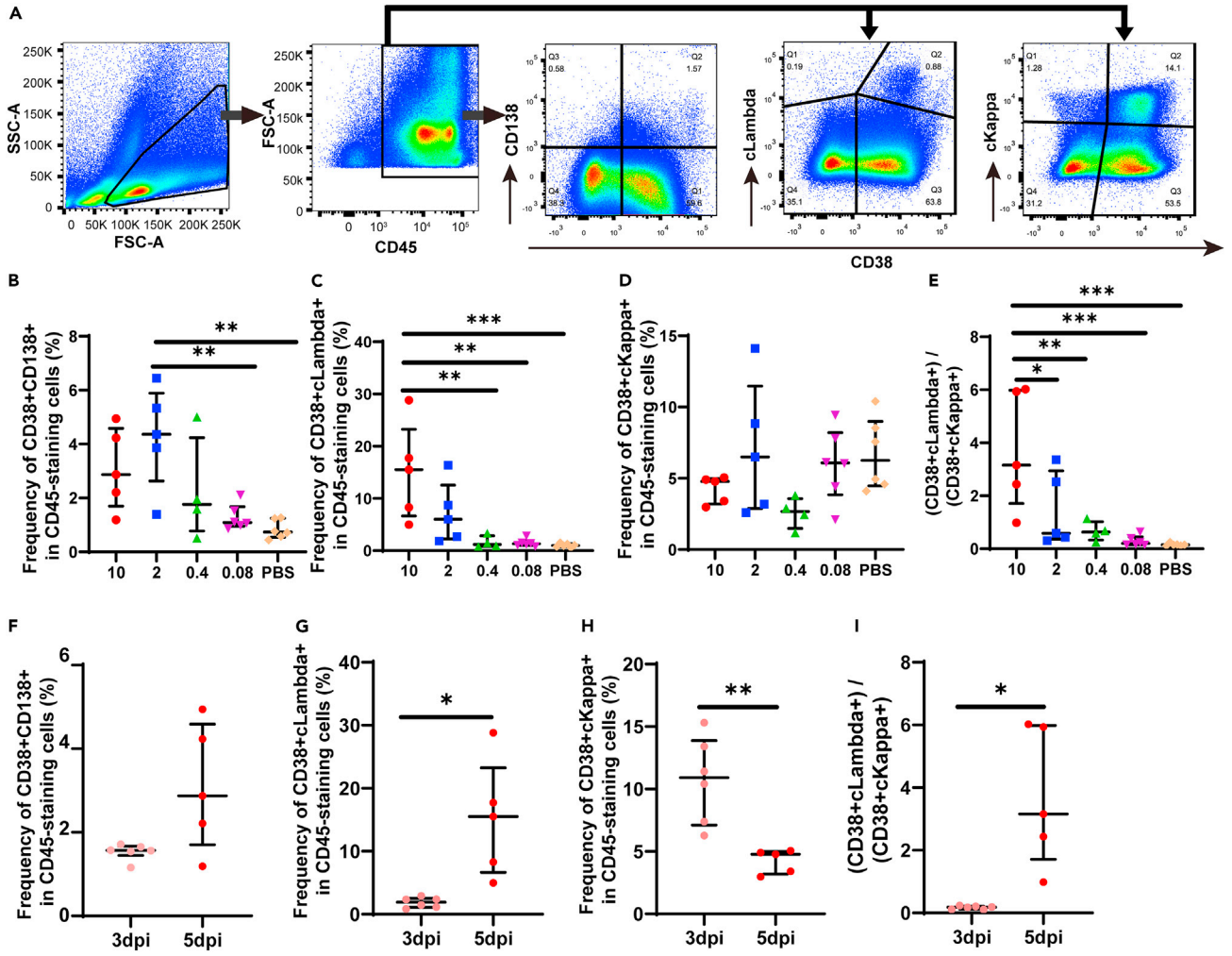

Figure 5. Monoclonal plasma cells overexpressing lambda light chain in different severe interferon receptor-deficient mouse bone marrow

(A) FACS gating strategy for measurements of plasma cell subsets in mice experiments.

(B) The frequency of $CD38^{+}CD138^{+}$ in different infection groups.

(C and D) The frequency of $CD38^{+}cLambda^{+}$ and $CD38^{+}cKappa^{+}$ plasma cells in bone marrow by intracellular staining, respectively.

(E) The ratio of $CD38^{+}cLambda^{+}/CD38^{+}cKappa$ in $CD45^{+}$ lymphocytes in different infection groups.

(F–I) The changes in different plasma cell subsets from 3 dpi to the 5 dpi in 10 PFU infection dose. Brown-Forsythe ANOVA tests with Holm-Sidak's multiple comparisons test were used for the analyses, and the differences between two groups were tested by *t* test. Sample data collected for phosphate-buffered saline (PBS), 0.08, 0.4, 2, and 10 PFU in 5 dpi. The median (IQR) is shown for each group, and statistical significance is represented by asterisks, *$p < 0.05$, **$p < 0.01$, ***$p < 0.001$; no significance was not shown for clear picture.

lambda-type plasma subsets was identified in eight SFTS patients, which were similar to that observed in lambda light chain multiple myeloma.[25] Collectively, this is a systematic report that SFTSV infection could cause overproliferation of monoclonal lambda-type plasma cells in the bone marrow, which enriches our understanding of viral pathogenesis and potentially inform the rational design of efficacious therapeutic treatments.

Identification of potential prognostic factors for a fatal outcome of SFTS is of great clinical significance. Previous studies have revealed that the concentrations of important biomarkers (including ALT, AST, CK, LDH, and D-dimer) in the acute phase are significantly higher in fatal cases than those in the survivors.[7,9,26] We discovered that the majority of the SFTS patients with monoclonal lambda-type plasma cells typically had higher concentrations of AST, ALT, LDH, and CK than those in the normal-plasma-cell group, suggesting potentially severe tissue injuries in the MCP patients. In particular, clinical symptoms and outcomes were

usually more severe in these cases, and half of the SFTS cases with MCP cells died. Therefore, the overproliferation of monoclonal lambda-type plasma cells may be correlated with clinical outcomes of SFTSV infection, which may serve as a potential prognostic biomarker for SFTS and aid in the development of therapeutics.

It is well established that viral infection can cause tumors, such as those induced by human papillomavirus high-risk types, Epstein-Barr virus, hepatitis B virus, and human T-lymphotropic virus type 1.[27] However, the overexpressed monoclonal lambda-type plasma cells in the recovered SFTS patients are clearly different from lambda light chain multiple myeloma as the overproliferation of monoclonal lambda-type plasma cells in the bone marrow of the SFTS patients appeared to be transient. Hence, caution should be exercised to avoid misdiagnosis of SFTSV and lambda light chain multiple myeloma or other blood diseases.[11,28]

Bone marrow examination has been previously employed in SFTS studies.[18,29] Cytological changes in the bone marrow of SFTS patients have been described as early as in 2013, which showed that there was no difference between the SFTS patients and healthy controls, but the SFTS patients had significant cytological variance with acute aplastic anemia patients.[30] Meanwhile, macrophage hematophilia was also found in the bone marrow of SFTS patients, especially in fatal cases.[8,18] Hemophagocytic histiocytosis has been also described in the bone marrow of SFTS cases,[31,32] which was also observed in bone marrow biopsy samples of four SFTS cases in this study. Importantly, we discovered a lambda light chain multiple myeloma-like plasma cell phenotype caused by SFTSV infection using bone marrow flow cytometry and IHC methods. Further, overproliferation of monoclonal lambda-type plasma cells were also found in animal experiments in the high-dose infection group, which suggested that SFTSV infection could cause overproliferation of monoclonal lambda-type plasma cells in bone marrow. Therefore, examination of bone marrow could shed light on understanding pathogenic mechanisms of SFTSV and potentially other high-consequence viral hemorrhagic infectious diseases.

Importantly, the mechanism(s) underlying the overproliferation phenotype of monoclonal lambda-type plasma cells in SFTS cases we have described remains unknown. It is well reported that viral infection can cause immunoblastic and polyclonal B cell activation, such as following Hantavirus, Epstein-Barr virus, and Dengue virus infection. However, it has been reported that the signaling through pattern-recognition receptors combined with certain cytokines is able to induce polyclonal activation of human memory B cells and subsequent differentiation into antibody-secreting cells.[33,34] In addition, B cells could constitute alternative target cells for the Andes orthohantavirus infection and lead to their polyclonal activation, as has been demonstrated for dengue virus.[35,36]

Interestingly, only the monoclonal lambda-type plasma cells were discovered in the bone marrow of the SFTS cases, and we did not find the kappa-type MCP cells, which was consistent with prior observations from peripheral blood mononuclear cells.[37] Hence, we speculate that a high viral load at the acute phase of SFTSV infection, mimicked by the high infectious dose in the animal model, may cause cellular metabolic disorders of B cells and thereby trigger lambda light chain expression, which clearly warrants further study. In addition, whether the presence of MCP cells affects the expression of neutralizing antibodies also requires further investigation. Importantly, half of the MCP cases died and the presence of MCP cells seemed to be closely related to both more severe clinical symptoms and outcomes in the present study.

In summary, we report that SFTSV infection can cause a transient overproliferation of monoclonal lambda-type plasma cells, which is related to clinical severity and infection outcome. Notably, this study sheds light on a tumor phenotype of SFTSV infection, which might represent a unique pathogenic mechanism of SFTS. Whether this phenotype is also found in other hemorrhagic infectious diseases and its correlation with disease severity warrant further detailed scientific and clinical investigation.

Limitations of the study

This study has several limitations. Firstly, when the proportion of the $CD38^{+}$ subset fell within the normal range (<0.5%), the plasma cell phenotypes were not analyzed so that only 9 out of the 22 SFTS cases with normal plasma cells were analyzed in more detail. Secondly, eight of the 30 SFTS patients exhibited overproliferation of MCP cells; however, only four MCP cases survived, and three cases were successfully followed up. Therefore, the sample size is small, and assessing whether MCP cells affect the secretion of effective viral-targeting monoclonal antibodies needs further study. Thirdly, we did not have serial samples

from fatal NP cases and failed to assess whether MCP cells also appear in the later infection period. Finally, the IFNα/βR$^{-/-}$ mouse model is different from humans, and other animal models such as humanized mice, ferrets, or cats were not used to validate the findings in patients.

STAR★METHODS

Detailed methods are provided in the online version of this paper and include the following:

- KEY RESOURCES TABLE
- RESOURCE AVAILABILITY
  - Lead contact
  - Materials availability
  - Data and code availability
- EXPERIMENTAL MODEL AND SUBJECT DETAILS
  - Cell lines and mice
  - Collection of clinical data and sample
  - Definition of monoclonal plasma cells among SFTS patients
  - Study approvals
- METHOD DETAILS
  - Determination of viral titers
  - Immunohistochemistry and immunofluorescence
  - Real-time reverse-transcription quantitative polymerase chain reaction
  - Measurement of SFTSV antibodies
  - Infections
  - Intracellular staining and flow cytometry
  - Phylogenetic analysis
- QUANTIFICATION AND STATISTICAL ANALYSIS
  - Statistical analysis

SUPPLEMENTAL INFORMATION

Supplemental information can be found online at https://doi.org/10.1016/j.isci.2023.106799.

ACKNOWLEDGMENTS

This work was supported by the Academic Promotion Program of Shandong First Medical University (Grant number 2019QL006), the Natural Science Foundation of Shandong Province (Grant number ZR2020QH133), the Youth Innovation Team of Shandong Higher Education Institution (Grant number 2021KJ064), the Medical and Health Technology Development Plan of Shandong (Grant number 202011001103), the Science and Technology Development Plan of Taian (Grant number 2021NS220), and the Taishan Scholars Programme of Shandong Province (Grant number tsqn202211217). We thank Dr. Jie Wei and Jianfeng Zhou, who worked in King Med Diagnosis, for helpful comments on this study.

AUTHOR CONTRIBUTIONS

W.S. and H.Z. designed and supervised this study. C.Q., Q.L., C.L., H.W., M.Y., and L.W. collected the samples and clinical data. C.Q., L.Y., K.N., G.D., H.Z., X.W., W.S., W.Z., Q.L., W.X., and Z.Z. performed experiments, analyzed the data, and performed the statistical analyses. W.S., H.Z., C.Q., L.Y., and G.D. interpreted the results and wrote the manuscript. W.S. and M.J.C. edited the manuscript. All authors had full access to all of the data in the study and accept responsibility for the decision to submit for publication.

DECLARATION OF INTERESTS

The authors declare no competing interests.

Received: October 8, 2022
Revised: April 7, 2023
Accepted: April 28, 2023
Published: May 4, 2023

REFERENCES

1. Wang, Y., Han, S., Ran, R., Li, A., Liu, H., Liu, M., Duan, Y., Zhang, X., Zhao, Z., Song, S., et al. (2021). A longitudinal sampling study of transcriptomic and epigenetic profiles in patients with thrombocytopenia syndrome. Nat. Commun. *12*, 5629. https://doi.org/10.1038/s41467-021-25804-z.

2. Yu, X.J., Liang, M.F., Zhang, S.Y., Liu, Y., Li, J.D., Sun, Y.L., Zhang, L., Zhang, Q.F., Popov, V.L., Li, C., et al. (2011). Fever with thrombocytopenia associated with a novel bunyavirus in China. N. Engl. J. Med. *364*, 1523–1532. https://doi.org/10.1056/NEJMoa1010095.

3. Tran, X.C., Yun, Y., Van An, L., Kim, S.H., Thao, N.T.P., Man, P.K.C., Yoo, J.R., Heo, S.T., Cho, N.H., and Lee, K.H. (2019). Endemic severe fever with thrombocytopenia syndrome, Vietnam. Emerg. Infect. Dis. *25*, 1029–1031. https://doi.org/10.3201/eid2505.181463.

4. Lin, T.L., Ou, S.C., Maeda, K., Shimoda, H., Chan, J.P.W., Tu, W.C., Hsu, W.L., and Chou, C.C. (2020). The first discovery of severe fever with thrombocytopenia syndrome virus in Taiwan. Emerg. Microbes Infect. *9*, 148–151. https://doi.org/10.1080/22221751.2019.1710436.

5. Kang, J.G., Cho, Y.K., Jo, Y.S., Chae, J.B., Joo, Y.H., Park, K.W., and Chae, J.S. (2019). Severe fever with thrombocytopenia syndrome virus in dogs, South Korea. Emerg. Infect. Dis. *25*, 376–378. https://doi.org/10.3201/eid2502.180859.

6. World Health Organization (2018). Annual review of diseases prioritized under the research and development blueprint informal consultation. https://www.who.int/news-room/events/detail/2018/02/06/default-calendar/2018-annual-review-of-diseases-prioritized-under-the-research-anddevelopment-blueprint.

7. Gai, Z.T., Zhang, Y., Liang, M.F., Jin, C., Zhang, S., Zhu, C.B., Li, C., Li, X.Y., Zhang, Q.F., Bian, P.F., et al. (2012). Clinical progress and risk factors for death in severe fever with thrombocytopenia syndrome patients. J. Infect. Dis. *206*, 1095–1102. https://doi.org/10.1093/infdis/jis472.

8. Hiraki, T., Yoshimitsu, M., Suzuki, T., Goto, Y., Higashi, M., Yokoyama, S., Tabuchi, T., Futatsuki, T., Nakamura, K., Hasegawa, H., et al. (2014). Two autopsy cases of severe fever with thrombocytopenia syndrome (SFTS) in Japan: a pathognomonic histological feature and unique complication of SFTS. Pathol. Int. *64*, 569–575. https://doi.org/10.1111/pin.12207.

9. Liu, Q., He, B., Huang, S.Y., Wei, F., and Zhu, X.Q. (2014). Severe fever with thrombocytopenia syndrome, an emerging tick-borne zoonosis. Lancet Infect. Dis. *14*, 763–772. https://doi.org/10.1016/S1473-3099(14)70718-2.

10. Li, J., Li, S., Yang, L., Cao, P., and Lu, J. (2021). Severe fever with thrombocytopenia syndrome virus: a highly lethal bunyavirus. Crit. Rev. Microbiol. *47*, 112–125. https://doi.org/10.1080/1040841X.2020.1847037.

11. Kaneko, M., Shikata, H., Matsukage, S., Maruta, M., Shinomiya, H., Suzuki, T., Hasegawa, H., Shimojima, M., and Saijo, M. (2018). A patient with severe fever with thrombocytopenia syndrome and hemophagocytic lymphohistiocytosis-associated involvement of the central nervous system. J. Infect. Chemother. *24*, 292–297. https://doi.org/10.1016/j.jiac.2017.10.016.

12. Li, X.K., Lu, Q.B., Chen, W.W., Xu, W., Liu, R., Zhang, S.F., Du, J., Li, H., Yao, K., Zhai, D., et al. (2018). Arginine deficiency is involved in thrombocytopenia and immunosuppression in severe fever with thrombocytopenia syndrome. Sci. Transl. Med. *10*, eaat4162. https://doi.org/10.1126/scitranslmed.aat4162.

13. Li, H., Li, X., Lv, S., Peng, X., Cui, N., Yang, T., Yang, Z., Yuan, C., Yuan, Y., Yao, J., et al. (2021). Single-cell landscape of peripheral immune responses to fatal SFTS. Cell Rep. *37*, 110039. https://doi.org/10.1016/j.celrep.2021.110039.

14. Xu, S., Jiang, N., Nawaz, W., Liu, B., Zhang, F., Liu, Y., Wu, X., and Wu, Z. (2021). Infection of humanized mice with a novel phlebovirus presented pathogenic features of sever fever with thrombocytopenia syndrome. PLoS Pathog. *17*.

15. Suzuki, T., Sato, Y., Sano, K., Arashiro, T., Katano, H., Nakajima, N., Shimojima, M., Kataoka, M., Takahashi, K., Wada, Y., et al. (2020). Severe fever with thrombocytopenia syndrome virus targets B cells in lethal human infections. J. Clin. Invest. *130*, 799–812. https://doi.org/10.1172/JCI129171.

16. Song, P., Zheng, N., Liu, Y., Tian, C., Wu, X., Ma, X., Chen, D., Zou, X., Wang, G., Wang, H., et al. (2018). Deficient humoral responses and disrupted B-cell immunity are associated with fatal SFTSV infection. Nat. Commun. *9*, 3328. https://doi.org/10.1038/s41467-018-05746-9.

17. Park, A., Park, S.J., Jung, K.L., Kim, S.M., Kim, E.H., Kim, Y.I., Foo, S.S., Kim, S., Kim, S.G., Yu, K.M., et al. (2021). Molecular signatures of inflammatory profile and B-Cell function in patients with severe fever with thrombocytopenia syndrome. mBio *12*, e02583-20. https://doi.org/10.1128/mBio.02583-20.

18. Kim, N., Kim, K.H., Lee, S.J., Park, S.H., Kim, I.S., Lee, E.Y., and Yi, J. (2016). Bone marrow findings in severe fever with thrombocytopenia syndrome: prominent haemophagocytosis and its implication in haemophagocytic lymphohistiocytosis. J. Clin. Pathol. *69*, 537–541. https://doi.org/10.1136/jclinpath-2015-203417.

19. Gupta, S., Karandikar, N.J., Ginader, T., Bellizzi, A.M., and Holman, C.J. (2018). Flow cytometric aberrancies in plasma cell myeloma and MGUS - correlation with laboratory parameters. Cytometry B Clin. Cytom. *94*, 500–508. https://doi.org/10.1002/cyto.b.21624.

20. Sun, Y., Jin, C., Zhan, F., Wang, X., Liang, M., Zhang, Q., Ding, S., Guan, X., Huo, X., Li, C., et al. (2012). Host cytokine storm is associated with disease severity of severe fever with thrombocytopenia syndrome. J. Infect. Dis. *206*, 1085–1094. https://doi.org/10.1093/infdis/jis452.

21. Kastritis, E., Terpos, E., Moulopoulos, L., Spyropoulou-Vlachou, M., Kanellias, N., Eleftherakis-Papaiakovou, E., Gkotzamanidou, M., Migkou, M., Gavriatopoulou, M., Roussou, M., et al. (2013). Extensive bone marrow infiltration and abnormal free light chain ratio identifies patients with asymptomatic myeloma at high risk for progression to symptomatic disease. Leukemia *27*, 947–953. https://doi.org/10.1038/leu.2012.309.

22. Kumar, S.K., Rajkumar, V., Kyle, R.A., van Duin, M., Sonneveld, P., Mateos, M.V., Gay, F., and Anderson, K.C. (2017). Multiple myeloma. Nat. Rev. Dis. Primers *3*, 17046. https://doi.org/10.1038/nrdp.2017.46.

23. Castillo, J.J., and Treon, S.P. (2019). What is new in the treatment of Waldenstrom macroglobulinemia? Leukemia *33*, 2555–2562. https://doi.org/10.1038/s41375-019-0592-8.

24. Gertz, M.A., and Dispenzieri, A. (2020). Systemic amyloidosis recognition, prognosis, and therapy: a systematic review. JAMA *324*, 79–89. https://doi.org/10.1001/jama.2020.5493.

25. International Clinical Cytometry Society. Flow cytometric testing for kappa and lambda light chains sponsored and reviewed by ICCS quality and standards committee. (Jan 15, 2018). https://www.cytometry.org/web/modules/Module%206.pdf.

26. He, F., Zheng, X., and Zhang, Z. (2021). Clinical features of severe fever with thrombocytopenia syndrome and analysis of risk factors for mortality. BMC Infect. Dis. *21*, 1253. https://doi.org/10.1186/s12879-021-06946-3.

27. Gaglia, M.M., and Munger, K. (2018). More than just oncogenes: mechanisms of tumorigenesis by human viruses. Curr. Opin. Virol. *32*, 48–59. https://doi.org/10.1016/j.coviro.2018.09.003.

28. Fisman, D.N. (2000). Hemophagocytic syndromes and infection. Emerg. Infect. Dis. *6*, 601–608. https://doi.org/10.3201/eid0606.000608.

29. Tang, L.V., and Hu, Y. (2021). Hemophagocytic lymphohistiocytosis after COVID-19 vaccination. J. Hematol. Oncol. *14*, 87. https://doi.org/10.1186/s13045-021-01100-7.

30. QuanTai, X., FengZhe, C., XiuGuang, S., and DongGe, C. (2013). A study of cytological changes in the bone marrow of patients with severe fever with thrombocytopenia syndrome. PLoS One *8*, e83020. https://doi.org/10.1371/journal.pone.0083020.

31. Janka, G.E. (2012). Familial and acquired hemophagocytic lymphohistiocytosis. Annu. Rev. Med. *63*, 233–246. https://doi.org/10.1146/annurev-med-041610-134208.

32. Prilutskiy, A., Kritselis, M., Shevtsov, A., Yambayev, I., Vadlamudi, C., Zhao, Q., Kataria, Y., Sarosiek, S.R., Lerner, A., Sloan, J.M., et al. (2020). SARS-CoV-2 infection-associated hemophagocytic lymphohistiocytosis. Am. J. Clin. Pathol. *154*, 466–474. https://doi.org/10.1093/ajcp/aqaa124.

33. Bernasconi, N.L., Traggiai, E., and Lanzavecchia, A. (2002). Maintenance of serological memory by polyclonal activation of human memory B cells. Science *298*, 2199–2202. https://doi.org/10.1126/science.1076071.

34. Pinna, D., Corti, D., Jarrossay, D., Sallusto, F., and Lanzavecchia, A. (2009). Clonal dissection of the human memory B-cell repertoire following infection and vaccination. Eur. J. Immunol. *39*, 1260–1270. https://doi.org/10.1002/eji.200839129.

35. Correa, A.R.V., Rosa Berbel, A.C.E., Papa, M.P., de Morais, A.T.S., Peçanha, L.M.T., and de Arruda, L.B. (2015). Dengue virus directly stimulates polyclonal B cell activation. PLoS One *10*, e0143391. https://doi.org/10.1371/journal.pone.0143391.

36. García, M., Iglesias, A., Landoni, V.I., Bellomo, C., Bruno, A., Córdoba, M.T., Balboa, L., Fernández, G.C., Sasiain, M.D.C., Martínez, V.P., and Schierloh, P. (2017). Massive plasmablast response elicited in the acute phase of hantavirus pulmonary syndrome. Immunology *151*, 122–135. https://doi.org/10.1111/imm.12713.

37. Takahashi, T., Suzuki, T., Hiroshige, S., Nouno, S., Matsumura, T., Tominaga, T., Yujiri, T., Katano, H., Sato, Y., and Hasegawa, H. (2019). Transient appearance of plasmablasts in the peripheral blood of Japanese patients with severe fever with thrombocytopenia syndrome. J. Infect. Dis. *220*, 23–27. https://doi.org/10.1093/infdis/jiz054.

38. Chinese Hematology Association; Chinese Society of Hematology; Chinese Myeloma Committee-Chinese Hematology Association (2020). The guidelines for the diagnosis and management of multiple myeloma in China (2020 revision). Zhonghua Nei Ke Za Zhi *59*, 341–346. https://doi.org/10.3760/cma.j.cn112138-20200304-00179.

39. Oka, S., Muroi, K., Sato, K., Fujiwara, S.i., Oh, I., Matsuyama, T., Ohmine, K., Suzuki, T., Ozaki, K., Mori, M., et al. (2012). Flow cytometric analysis of kappa and lambda light chain expression in endoscopic biopsy specimens before the diagnosis of B-cell lymphoma. J. Clin. Exp. Hematop. *52*, 127–131. https://doi.org/10.3960/jslrt.52.127.

40. Sun, Y., Liang, M., Qu, J., Jin, C., Zhang, Q., Li, J., Jiang, X., Wang, Q., Lu, J., Gu, W., et al. (2012). Early diagnosis of novel SFTS bunyavirus infection by quantitative real-time RT-PCR assay. J. Clin. Virol. *53*, 48–53. https://doi.org/10.1016/j.jcv.2011.09.031.

41. Zhao, M., Liu, K., Luo, J., Tan, S., Quan, C., Zhang, S., Chai, Y., Qi, J., Li, Y., Bi, Y., et al. (2018). Heterosubtypic protections against human-infecting avian influenza viruses correlate to biased cross-T-cell responses. mBio *9*, e01408-18. https://doi.org/10.1128/mBio.01408-18.

42. Bi, Y., Tan, S., Yang, Y., Wong, G., Zhao, M., Zhang, Q., Wang, Q., Zhao, X., Li, L., Yuan, J., et al. (2019). Clinical and immunological characteristics of human infections with H5N6 avian influenza virus. Clin. Infect. Dis. *68*, 1100–1109. https://doi.org/10.1093/cid/ciy681.

43. Edgar, R.C. (2004). MUSCLE: multiple sequence alignment with high accuracy and high throughput. Nucleic Acids Res. *32*, 1792–1797. https://doi.org/10.1093/nar/gkh340.

44. Minh, B.Q., Schmidt, H.A., Chernomor, O., Schrempf, D., Woodhams, M.D., von Haeseler, A., and Lanfear, R. (2020). IQ-TREE 2: new models and efficient methods for phylogenetic inference in the genomic Era. Mol. Biol. Evol. *37*, 1530–1534. https://doi.org/10.1093/molbev/msaa015.

45. Wu, X., Li, M., Zhang, Y., Liang, B., Shi, J., Fang, Y., Su, Z., Li, M., Zhang, W., Xu, L., et al. (2021). Novel SFTSV phylogeny reveals new reassortment events and migration routes. Virol. Sin. *36*, 300–310. https://doi.org/10.1007/s12250-020-00289-0.

46. Lv, Q., Zhang, H., Tian, L., Zhang, R., Zhang, Z., Li, J., Tong, Y., Fan, H., Carr, M.J., and Shi, W. (2017). Novel sub-lineages, recombinants and reassortants of severe fever with thrombocytopenia syndrome virus. Ticks Tick. Borne. Dis. *8*, 385–390. https://doi.org/10.1016/j.ttbdis.2016.12.015.

STAR★METHODS

KEY RESOURCES TABLE

REAGENT or RESOURCE	SOURCE	IDENTIFIER
Antibodies		
Anti-human CD19	MXB Blotechnologles	Cat# clone MX016
PE/Cyanine7 anti-mouse CD19	Biolegend	Cat# clone 6D9; RRID:AB_2927870
Anti-human CD20	MXB Blotechnologles	Cat# clone L26
Anti-human CD38	MXB Blotechnologles	Cat# clone MX044
Anti-human CD38	Proteintech	Cat# clone 3C6G4
Brilliant Violet 421 anti-mouse CD38	Biolegend	Cat# clone 90; RRID:AB_2734153
Brilliant Violet 711 anti-mouse CD45	Biolegend	Cat# clone 30-F11; RRID:AB_2564383
Anti-human CD138	MXB Blotechnologles	Cat# clone MI15
PerCP/Cyanine5.5 anti-mouse CD138	Biolegend	Cat# clone 281-2; RRID:AB_2561600
Multi-clonal anti-human kappa	MXB Blotechnologles	Cat# clone RAB-0111
Multi-clonal anti-human lambda	MXB Blotechnologles	Cat# clone LAM03+ HP6054
Multi-clonal anti-human lambda	Proteintech	Cat# clone 20758-1-AP
FITC anti-mouse kappa	Biolegend	Cat# clone RMK-48; RRID:AB_2563584
PE anti-mouse lambda	Biolegend	Cat# clone RML-42; RRID:AB_1027660
DAB Kit	MXB Blotechnologles	Cat# DAB-0031
CoraLite488-conjugated goat anti-rabbit IgG(H + L)	Proteintech	Cat# Sa00013-2; RRID:AB_2797132
Coralite 594–conjugated goat anti-mouse IgG (H + L)	Solarbio	Cat# K1031G-AF594
Critical commercial assays		
Cytofix/Cytoperm	BD	Cat# 554714
MagaBio plus Virus RNA Purification Kit	BIOER	Cat# BSC86S1E
ReverTra Ace® qPCR RT Kit	TOYOBO	Cat# FSQ101
Trans-Start Top Green qPCR Super-Mix	TRAN	Cat# AQ131
SFTSV IgM elisa kit	Daan Gene	N/A
SFTSV IgG elisa kit	Daan Gene	N/A
Experimental models: Cells, media, and virus		
SFTSV strain SDTA-1	In-house	GenBank: KX641909
Vero cells	In-house	N/A
Dulbecco's Modified Eagle Medium	Gibco	Cat# C11995500BT
Fetal bovine serum	Gibco	Cat# 10437-028
Penicillin-streptomycin	Solarbio	Cat# P1400
Red blood lysis solution	Solarbo	Cat# R1016
Interferon alpha/beta receptor gene-deficient A129 mice	In-house	N/A
Biological samples		
Blood	the Second Affiliated Hospital of Shandong First Medical University	N/A
Bone marrow biopsy and aspiration	the Second Affiliated Hospital of Shandong First Medical University	N/A

(*Continued on next page*)

Continued

REAGENT or RESOURCE	SOURCE	IDENTIFIER
Deposited data		
SFTSV sequence	This paper	GenBank: OP379659-OP379665, OP379667-OP379673, and OP379675-OP379681
Single-cell RNA-seq data	This paper	GSA: HRA004330
Software and algorithms		
Prism 8	GraphPad	https://www.graphpad.com/
R package	R CRAN	https://www.r-project.org/
Seurat v4	Satija Lab and Collaborators	https://satijalab.org/seurat/
FlowJo 10	Treestar	https://www.flowjo.com/solutions/flowjo

RESOURCE AVAILABILITY

Lead contact

Further information and requests for resources and reagents should be directed to and will be fulfilled by the lead contact, Weifeng Shi (shiwf@ioz.ac.cn).

Materials availability

All requests for resources and reagents should be directed to the lead contact author. All reagents will be made available on request after completion of a Materials Transfer Agreement.

Data and code availability

- Full-length genome sequences of the seven SFTSV generated in our study have been deposited in the GenBank under accession numbers OP379659-OP379665, OP379667-OP379673, and OP379675-OP379681. Single-cell RNA-seq data have been deposited into the GSA database under accession number HRA004330.
- This paper does not report original code.
- Any additional information required to reanalyze the data reported in this paper is available from the lead contact upon request.

EXPERIMENTAL MODEL AND SUBJECT DETAILS

Cell lines and mice

Vero cells were maintained in dulbecco's modified eagle medium (DMEM) containing 10% fetal bovine serum at 37°C with 5% CO_2. Interferon alpha/beta receptor gene-deficient A129 mice were obtained from School of Medicine, Tsinghua University, and maintained at the Key Laboratory of Etiology and Epidemiology of Emerging Infectious Diseases in Universities of Shandong, Shandong First Medical University. Since the sex ratio in the MCP group is 1:1, we selected 8 to 12-week-old female or male mice for virus challenge. All animal handling procedures were performed in compliance with the People's Republic of China legislation for the care and use of laboratory animals. The experiments and protocol were approved by the Committee on the Ethics of Animal Experiments of Shandong First Medical University & Shandong Academy of Medical Sciences under permit W202103030180.

Collection of clinical data and sample

Outpatients with suspected SFTS, including fever, history of tick bites, thrombocytopenia, and clinical presentation during the SFTS season (March to October), were enrolled at the Second Affiliated Hospital of Shandong First Medical University between April 2018 and May 2022. The patients were examined for SFTSV infection by quantitative RT-PCR, antibody testing, or high-throughput sequencing, and simultaneously the routine testing for hematopoiesis were used for further analysis. Individuals were omitted from the study based on the following exclusion criteria: (1) suspected cases without marrow examination; (2) suspected cases without antibody or sequencing results; (3) antibody or sequencing findings were negative in suspected cases; (4) cases were diagnosed with acute myeloid leukemia or monoclonal B cell

proliferation. The clinical outcomes of SFTS patients obtained from hematological analysis and urinalysis were regularly recorded, as well as the cell subtype information in bone marrow, so as to exclude hematologic diseases, were also collected for data analysis. The plasma and sera were separated and stored at −80°C until further testing.

Definition of monoclonal plasma cells among SFTS patients

The monoclonal plasma cell overproliferation among SFTS patients was similar with the clonal plasma cell in certain multiple myeloma phenotypes. According to the diagnosis and treatment standard of multiple myeloma in China (revised in 2022),[38] the multiple myeloma patients were enrolled as a control group. Briefly, the multiple myeloma diagnosis was based on the ratio of clonal plasma cells, serum calcium, anemia, bone lesions: clonal bone marrow plasma cells ≥10% or biopsy-proven bone or extramedullary plasmacytoma and anyone or more of the following myeloma-defining events: (1) monoclonal protein in serum or urine; (2) hypercalcaemia >2.75 mmol/L; (3) renal insufficiency: serum creatinine >177 mmol/L; (4) anemia: a hemoglobin value <100 g/L; (5) bone lesions: one or more osteolytic lesions on skeletal radiography, X-ray film, computed tomography, magnetic resonance imaging, or positron emission tomography-computed tomography. Further, the MCP cells among SFTS patients were defined according to the ratio of $CD38^+cLambda^+$: $CD38^+cKappa^+$ is <1:3 (kappa type) or >3:1 (lambda type), and the normal plasma defined with ratios between 1:3 and 3:1.[24,39]

Study approvals

This study was approved by the ethics committee of the Shandong First Medical University & Shandong Academy of Medical Sciences (R2021030300920). The study followed the principles of the Declaration of Helsinki, and the standards of Good Clinical Practice as defined by the International Conference on Harmonization (https://www.ich.org). Written informed consent was obtained from each enrolled case. The research-related information was used anonymously.

METHOD DETAILS

Determination of viral titers

The SFTSV strain SDTA-1 (GenBank: KX641909) was propagated in Vero cells with DMEM supplemented with 1% fetal bovine serum and penicillin-streptomycin for five days. The 50% tissue culture infectious dose ($TCID_{50}$) values of SDTA-1 were titrated on Vero cells using the Reed-Muench method. The supernatant was diluted by 10-fold serial dilution with DMEM, which was transferred to pre-prepared Vero cells in 96-well plates and incubated for 96 h. The viruses in 96-well plates were fixed and permeabilized with cooled absolute ethanol for 20 min at 4°C. Vero cells were stained with humanized Gn-IgG antibody at 10 μg/mL, followed by Alexa Fluor 488-conjugated goat anti-human Ig antibody at 1:200. The double IF staining was visualized and calculated employing ZEISS observer 300 (Germany).

Immunohistochemistry and immunofluorescence

Formalin-fixed, paraffin-embedded (FFPE) human marrow tissues from SFTS cases were examined. All FFPE tissues were cut into 3-μm-thick sections. Immunohistochemistry for host-cell proteins was performed with anti-CD19, anti-CD20, anti-CD38, anti-CD138, multi-clonal anti-kappa from rabbits, and multi-clonal anti-lambda from mice. Immunofluorescence for host-cell proteins was performed with anti-CD38, anti-human IgG lambda light chain polyclonal antibody, Coralite 488–conjugated affinipure anti–Rabbit IgG and Coralite 594–conjugated goat anti-mouse IgG (H + L) were used as secondary antibodies. Immunostaining was visualized by 3,3′-diaminobenzidine tetrahydrochloride (DAB) staining. DAB Chromogen Kit were used as chromogens for horseradish peroxidase visualization. The double IF staining was visualized with ZEISS observer 300 (Germany).

Real-time reverse-transcription quantitative polymerase chain reaction

The viral load was measured on plasma collected from patients at first hospitalization and in the mouse model. Viral RNA was extracted with MagaBio plus Virus RNA Purification Kit, and cDNA synthesis was performed using the ReverTra Ace qPCR RT Kit. SYBR Green-based real-time PCR assay (SYBR-qPCR) was performed by Trans-Start Top Green qPCR Super-Mix with the oligonucleotide primers as previously described.[40]

Measurement of SFTSV antibodies

Plasma or serum titers of IgM and IgG to SFTSV nucleocapsid protein (NP) were measured using commercial ELISA kits (Daan Gene, China) following the manufacturer's instructions. For neutralization, Vero cells in DMEM supplemented with 10% FBS and 1% penicillin-streptomycin were seeded at 40,000 cells per well into clear-bottom, white-walled 48-well plates and cultured overnight at 37°C. Equal volumes of heat-inactivated serum or plasma, and virus diluted to 100 $TCID_{50}$ were added together and incubated at 37°C for 1 h. The 400 μL mixture was transferred to a confluent layer of Vero cells and incubated for 3 h, then washed three times, and cultured at 37°C for 96 h with 5% CO_2. The results were directly determined by the SYBR-qPCR assay, and the cut-off value was $Ct \leq 30$. Serum samples were tested with a starting dilution of 1:20, followed by 2-fold serial dilutions to 1:640. The GMT was calculated as the reciprocal of the serum dilution, and the negative was designated as 5. In each assay, negative and positive control samples and virus back titrations were utilized to confirm the testing system stability.

Infections

Different infectious doses (10, 2, 0.4, 0.08 PFU/mL) of SDTA-1 strain in 200 μL PBS were inoculated in 8- to 12-week-old female or male IFNα/βR$^{-/-}$ gene-deficient A129 mice by an intraperitoneal injection route. The same operation was performed on the control group of mice with 200 μL of PBS. Body weight and survival of mice were monitored until 9 days post-infection.

To evaluate the occurrence of MCPs after SFTSV infection was related with infectious doses, the mice were divided into five groups and challenged with lethal 10 PFU to asymptomatic 0.08 PFU, including 10 PFU, 2 PFU, 0.4 PFU, 0.08 PFU, and PBS, and they were killed on day 5. Meanwhile, additional 6 mice were infected with 10 PFU and euthanized on day 3.

The main virus-targeted organs including blood, brain, intestine, and liver, based on previous reports, were collected and stored at −80°C. These organs were homogenized in 1 mL of PBS using a homogenizer (60 Hz/s) at 4°C. Then, solid debris was pelleted by centrifugation at 12,000 × *g* for 1 min, and the supernatant was used for virus testing. The bone marrow lymphocytes were repeatedly blown through a 1 mL syringe and mouse splenocytes were obtained by gently grinding moistened spleen sections. Lymphocytes were filtered through cell strainers and were lysed with red blood lysis solution to remove erythrocytes for 10 min in ice.[41] These cells were cryopreserved in liquid nitrogen before analysis.[18]

Intracellular staining and flow cytometry

Lymphocytes of infected mice bone marrow were recovered and stained with a panel of surface MAbs in fluorescence-activated cell sorter (FACS) buffer (0.5% bovine serum albumin) for 30 min on ice, including anti–CD19-PE-Cy7, anti–CD38-DAPI, anti–CD45-BV711, anti–CD138-Percp-Cy5.5 surface markers. The cells were then fixed and incubated in permeabilizing buffer, and then stained with anti–kappa–PE and anti–lambda–FITC. All fluorescent lymphocytes were gated on a flow cytometer AriaIII (BD Biosciences) and analyzed with FlowJo software.[42]

Phylogenetic analysis

The complete L, M, and S gene segments of SFTSV strains were downloaded from GenBank and used as reference strains, including 150 L gene sequences, 166 M gene sequences, and 155 S gene sequences. Multiple sequence alignment of three gene segments was performed using Muscle (version 5).[43] Phylogenetic analyses were performed using IQ-TREE2 (version 1.6.12).[44] Trees were visualized using FigTree (version 1.4.2). The classification of the SFTSV genotypes followed previous studies.[45,46]

QUANTIFICATION AND STATISTICAL ANALYSIS

Statistical analysis

All statistical analyses were conducted with GraphPad Prism (version 8.2.1, GraphPad Software, Inc.), and R (version 4.0, The R Foundation for Statistical Computing). The normality of continuous variables was examined by using the Shapiro-Wilk test. Continuous variables were expressed as mean ± standard deviation (SD) and median (IQR), as appropriate. Categorical variables were presented as a rate. GMT and its SD were described for NP-specific IgM/IgG and neutralizing antibodies. The differences between two groups and between multiple groups were tested by *t*-test and one-way analysis of variance (ANOVA) with Tukey's multiple comparisons (if equal variances were not assumed, Brown-Forsythe ANOVA test with

Games-Howell's multiple comparisons was used) for normally distributed data, respectively. Mann-Whitney test and Kruskal-Wallis test were used for non-normally distributed or discrete variables. Paired *t*-test was conducted to compare the levels of plasma cells in follow-up SFTS patients. *Spearman* correlation was adopted to examine the relationship between monoclonal plasma subsets and clinical severity in the SFTS patients. The survival curves of animal experiment were generated with a log rank (Mantel-Cox) test. Body weight rate of mice was analyzed with repeated measures ANOVA. $p < 0.05$ was considered statistically significant (*$p < 0.05$; **$p < 0.01$; ***$p < 0.001$).